Progress in Flight Dynamics, GNC, and Avionics **6** (2013) 545-568
DOI: 10.1051/eucass/201306545

SATELLITE LAUNCHER POINTING FOR ORBIT INJECTION WITH UNCONTROLLED SOLID-PROPELLANT LAST STAGE

A. de Lima Nepomuceno and W. de Castro Leite Filho

Instituto de Aeronáutica e Espaço
50 Praça Eduardo Gomes, Sao José dos Campos-SP 12228-904, Brasil

An orbit injection method is suggested for satellite launchers with an uncontrolled last stage, addressing both orbit plane geometry and inclination issues. An impulsive approach is used to model the transfer to an orbit, with last stage burning synchronized through its thrust acceleration profile. The method is also supported by strong in-flight identification of suborbital trajectory parameters, and feasibility preevaluation within fault conditions and requirements priorities. An iterative procedure determines, to the chosen precision, the parameters values needed to provide the best feasible orbit injection. Simulation tests results are used to demonstrate the good performance and reliability of the method.

1 INTRODUCTION

Following the initial propelled ascending phases and already beyond atmosphere, the considered launcher vehicle goes on a Keplerian suborbital trajectory phase, with attitude control capability. Along this suborbital trajectory, the vehicle must be positioned and stabilized in an adequate inertial longitudinal angular attitude in order to start, at an appropriate time, the transferring into the satellite final orbit, through the propulsion of an uncontrolled (no control on thrust intensity and direction) last stage. The satellite orbit is required to have a given inclination and a given eccentricity. An onboard pointing algorithm is used to provide values of the vehicle's longitudinal attitude and propulsion start-up time so that the satellite is injected into an orbit with the required inclination and eccentricity.

The method presented here is a pointing algorithm based on the concept of impulsive orbit transfer [1], where there are the parameters impulsive transfer ray, or impulse ray, and impulsive transfer time, or impulse time. This impulse ray becomes the orbit injection ray; and this impulse time becomes a reference

to fix the last-stage start-up time. It is considered that the orbit transfer is to be done by the target orbit perigee. Locally, the vehicle longitudinal attitude is specified by local pitch and yaw angles. A procedure is provided to calculate the impulse ray, local pitch angle, and timing using a fixed value of the local yaw angle. Another procedure calculates the local yaw angle and recalculates the local pitch angle, using a fixed value of the impulse ray. Hence, these procedures are executed alternately and iteratively, until the calculated values converge according to the chosen convergence criteria. By construction of the method, there is convergence in any situation, with a low limit in the number of iterations.

2 POINTING METHOD DEVELOPMENT

2.1 Orbit Transfer Synchronization

Impulsive orbit transfer is associated with an impulse time t_i, at which the transfer occurs instantaneously. But the time interval τ of propulsion during the transfer is finite. Therefore, the time t_0, at which the propulsion should begin, must be determined. The following data about the solid-propellant last stage used for the orbit transfer are considered:

τ — time interval of propulsion;
m_c — total mass of components (excluding propellant);
$m_p(t)$, $0 \le t \le \tau$, — time-varying propellant mass profile;
$T(t)$, $0 \le t \le \tau$, — time-varying vacuum thrust profile;
$A_p(t)$, $0 \le t \le \tau$, — time-varying propulsion acceleration profile; and
$\Delta V_p = \| \Delta \mathbf{V}_p \|$ — speed increment, or characteristic speed, due to propulsion.

Figure 1 illustrates the orbit transfer.

Vacuum conditions may be assumed because atmospheric pressure is negligible during the transfer. In the course of the actuation of the engine, the inertial direction of propulsion and of the resulting acceleration are constant. Here,

$$\Delta V_p = \int_0^\tau A_p(t)\, dt\,. \tag{1}$$

As a vacuum propulsion and propellant mass table of variation in time is available, numeric integration is quite convenient. This way, the acceleration has the following calculus, along with integration:

$$A_p(t) = \frac{T(t)}{m_c + m_p(t)}\,.$$

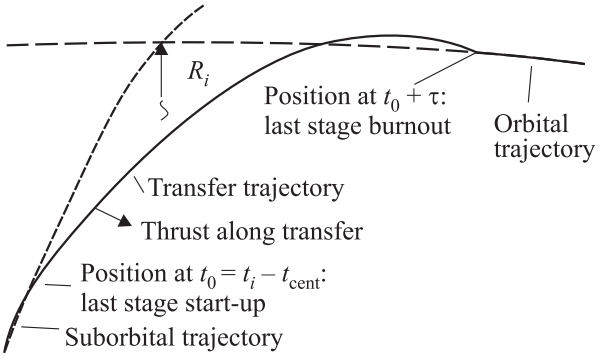

Figure 1 Synchronization of orbit transfer by centroid time of thrust acceleration profile

After integration, the centroid time t_{cent} of thrust acceleration profile is:

$$t_{\text{cent}} = \frac{\int_0^{\tau} tA_p(t)\,dt}{\int_0^{\tau} A_p(t)\,dt} = \frac{\int_0^{\tau} tA_p(t)\,dt}{\Delta V_p}\,. \tag{2}$$

Using this centroid time t_{cent}, the start-up time is set referred to the impulse time t_i [1] as $t_0 = t_i - t_{\text{cent}}$.

However, when fixing the start-up time t_0, its feasibility must be verified. Before the last stage start-up, the vehicle must be positioned and stabilized in the adequate inertial longitudinal angular attitude, the tipping maneuver. The time interval to do this is set as a constant for the mission and is named t_{tip}. If Dt_at_0 and Dt_at_i are the time intervals from the initial time t_a of the suborbital trajectory, respectively, till start-up time t_0 and impulse time t_i, it is required that

$$Dt_at_0 \geq t_{\text{tip}} \rightarrow Dt_at_i \geq t_{\text{tip}} + t_{\text{cent}}\,. \tag{3}$$

Usually, Eq. (3) is satisfied at the first setting of t_i. But if it is not, t_i and t_0 are revalued, as in subsections 2.4 and 2.5.

2.2 Reference Systems

To identify the suborbital, its parameters must be referred to an inertial geocentric equatorial reference frame. Here, this is also the inertial navigation frame **G**, with axes **XG**, **YG**, **ZG**, with **ZG** pointing to the North Pole.

For quantification of the pointing angles, an inertial reference frame **V**, with axes **XV**, **YV**, **ZV**, is determined by the inertial position and velocity vectors, as provided by navigation at initial time t_a when already in suborbital trajectory. Axis **XV** is aligned to this position vector and **XV** and **ZV** are in the suborbital trajectory plane; therefore, **YV** is normal to this plane. For transformations $\mathbf{V} \rightarrow \mathbf{G}$, a direction cosine matrix, called **TGV**, is used. This matrix is set by the coordinates in the frame **G** of the unit vectors of the frame **V** axes, taken as column vectors:

$$\left.\begin{aligned} \hat{\mathbf{x}}\mathbf{v}_\mathbf{G} = \frac{\mathbf{R}_{a\mathbf{G}}}{\parallel \mathbf{R}_{a\mathbf{G}} \parallel}\,; \quad \hat{\mathbf{y}}\mathbf{v}_\mathbf{G} = \frac{\mathbf{D}}{\parallel \mathbf{D} \parallel}\,; \quad \hat{\mathbf{z}}\mathbf{v}_\mathbf{G} = \frac{\mathbf{R}_{a\mathbf{G}} \times \mathbf{D}}{\parallel \mathbf{R}_{a\mathbf{G}} \times \mathbf{D} \parallel}\,; \\ \mathbf{TVG} = (\hat{\mathbf{x}}\mathbf{v}_\mathbf{G} \;\; \hat{\mathbf{y}}\mathbf{v}_\mathbf{G} \;\; \hat{\mathbf{z}}\mathbf{v}_\mathbf{G}) \end{aligned}\right\} \tag{4}$$

where $\mathbf{R}_{a\mathbf{G}}$ is the position at the initial time t_a in suborbital trajectory, expressed in the frame **G**; $\mathbf{D} = \mathbf{V}_{a\mathbf{G}} \times \mathbf{R}_{a\mathbf{G}}$; and $\mathbf{V}_{a\mathbf{G}}$ is the velocity at the initial time t_a in suborbital trajectory, expressed in the frame **G**.

One more inertial reference frame, the frame **I** with axes **XI**, **YI**, **ZI**, is utilized to set the vector relations for an impulsive transfer. Axis **XI** is aligned to the geocentric radial position vector $\mathbf{R}_i$ of the vehicle at the impulse time t_i. Axes **XI** and **ZI** are in the suborbital trajectory plane, and **YI** has the same orientation as **YV**. Transformation from frame **I** to frame **V** is performed through a simple rotation around **YI** or **YV**, at an angle equal to the difference between true anomalies $f_i - f_a$, geocentric angular displacement of the vehicle, from time t_a to time t_i.

2.3 Suborbital Trajectory Identification

Just after the suborbital trajectory is initiated, navigation provides the inertial position $\mathbf{R}_{a\mathbf{G}}$ ($R_a = \parallel \mathbf{R}_{a\mathbf{G}} \parallel$) and the velocity $\mathbf{V}_{a\mathbf{G}}$ ($V_a = \parallel \mathbf{V}_{a\mathbf{G}} \parallel$) expressed in the frame **G** and referred to the initial time t_a of this trajectory. The vector parameters specific angular momentum $\mathbf{H}_{\mathbf{sub_G}}$ ($H_{\text{sub}} = \parallel \mathbf{H}_{\mathbf{sub_G}} \parallel$), nodal $\mathbf{N}_{\mathbf{sub_G}}$ ($N_{\text{sub}} = \parallel \mathbf{N}_{\mathbf{sub_G}} \parallel$), and the eccentricity $\mathbf{e}_{\mathbf{sub_G}}$ ($e_{\text{sub}} = \parallel \mathbf{e}_{\mathbf{sub_G}} \parallel$), constants for the suborbital trajectory and expressed in the frame **G**, are [2]:

$$\left.\begin{aligned} \mathbf{H}_{\mathbf{sub_G}} = \left(H_{\text{sub}_{\mathbf{Gx}}} \; H_{\text{sub}_{\mathbf{Gy}}} \; H_{\text{sub}_{\mathbf{Gz}}}\right)^{\mathrm{T}} = \mathbf{R}_{a\mathbf{G}} \times \mathbf{V}_{a\mathbf{G}}\,; \\ \mathbf{N}_{\mathbf{sub_G}} = (0\;0\;1)^{\mathrm{T}} \times \mathbf{H}_{\mathbf{sub_G}} = \left(-H_{\text{sub}_{\mathbf{Gy}}} \; H_{\text{sub}_{\mathbf{Gx}}} \; 0\right)^{\mathrm{T}}\,; \end{aligned}\right\} \tag{5}$$

$$\begin{aligned} \mathbf{e}_{\mathbf{sub_G}} &= \left(e_{\text{sub}_{\mathbf{Gx}}} \;\; e_{\text{sub}_{\mathbf{Gy}}} \;\; e_{\text{sub}_{\mathbf{Gz}}}\right)^{\mathrm{T}} \\ &= \frac{1}{\mu}\left[\left(V_a^2 - \frac{\mu}{R_a}\right)\mathbf{R}_{a\mathbf{G}} - (\mathbf{R}_{a\mathbf{G}} \cdot \mathbf{V}_{a\mathbf{G}})\,\mathbf{V}_{a\mathbf{G}}\right] \end{aligned} \tag{6}$$

where μ is the Earth gravitational parameter.

Also constant for the suborbital, the scalar parameters semimajor axis a_{sub}, semilatus rectum p_{sub}, apogee ray R_{aposub}, apogee speed V_{aposub}, mean motion n_{sub}, inclination I_{sub}, and the argument of perigee ω_{sub} are [2]:

$$a_{\text{sub}} = \frac{R_a}{2 - R_a V_a^2/\mu}\,; \tag{7}$$

$$p_{\text{sub}} = a_{\text{sub}}\left(1 - e_{\text{sub}}^2\right)\,; \tag{8}$$

$$R_{\text{aposub}} = a_{\text{sub}}\left(1 + e_{\text{sub}}\right)\,; \tag{9}$$

$$V_{\text{aposub}} = \left(\frac{\mu}{p_{\text{sub}}}\right)^{1/2}\left(1 - e_{\text{sub}}\right)\,; \tag{10}$$

$$n_{\text{sub}} = \left(\frac{\mu}{a_{\text{sub}}^3}\right)^{1/2}\,; \tag{11}$$

$$I_{\text{sub}} = \arccos\left(\frac{H_{\text{sub}_{\mathbf{Gz}}}}{H_{\text{sub}}}\right)\,; \tag{12}$$

$$\cos\left(\omega_{\text{sub}}\right) = \frac{\mathbf{e_{sub_G}} \cdot \mathbf{N_{sub_G}}}{e_{\text{sub}} N_{\text{sub}}} \tag{13}$$

where if $e_{\text{sub}_{\mathbf{Gz}}} > 0$, then $0 \leq \omega_{\text{sub}} < \pi$; else $\pi \leq \omega_{\text{sub}} < 2\pi$.

The time-varying parameters trajectory angle β_a, true anomaly f_a, and eccentric anomaly E_a for the time t_a in suborbital trajectory are [2]:

$$\beta_a = \arcsin\left(\frac{\mathbf{R}_{a\mathbf{G}} \cdot \mathbf{V}_{a\mathbf{G}}}{R_a V_a}\right)\,; \tag{14}$$

$$\cos(f_a) = \frac{p_{\text{sub}} - R_a}{e_{\text{sub}} R_a}\,; \tag{15}$$

$$\cos(E_a) = \frac{a_{\text{sub}} - R_a}{a_{\text{sub}} e_{\text{sub}}} \tag{16}$$

where if $\beta_a \geq 0$, then $0 \leq f_a \leq \pi$ and $0 \leq E_a \leq \pi$; else $\pi < f_a < 2\pi$ and $\pi < E_a < 2\pi$.

The trajectory angle β_a in Eq. (14) is to be positive. If not, then the vehicle is entering the suborbital trajectory already in decreasing altitude, and this is treated as fault condition. But if β_a is positive as expected, the time interval $Dt_a t_{\text{aposub}}$, from t_a till apogee time t_{aposub}, is [2]:

$$Dt_a t_{\text{aposub}} = \frac{1}{n_{\text{sub}}}\left[\pi - E_a + e_{\text{sub}} \sin\left(E_a\right)\right]\,. \tag{17}$$

2.4 Solution Constraints and Requirements Priority

The vehicle's initial propelled stages are planned so that it enters the suborbital trajectory under conditions being such that the orbit requirements can be fully

satisfied through the transfer stage. However, the possibility of dispersions in initial phases that lead to the impossibility of requirements fulfillment must be considered. If this occurs, the best feasible solution is determined, taking into account a preestablished priority between inclination and eccentricity requirements. It should be kept in mind that orbit transfer is to be done by the target orbit perigee. The following variables are set:
$R_{i\mathrm{bot}}$ — minimum impulse ray allowing orbit transfer by perigee;
h_{aposub} — altitude of the suborbital trajectory apogee, corresponding to its apogee ray R_{aposub} in Eq. (9);
$R_{i\mathrm{top}}$ — maximum possible impulse ray;
$Dt_a t_{i\mathrm{top}}$ — time interval from initial time t_a till time corresponding to $R_{i\mathrm{top}}$, in the suborbital trajectory;
$E_{i\mathrm{top}}$ — eccentric anomaly corresponding to $R_{i\mathrm{top}}$;
$f_{i\mathrm{top}}$ — true anomaly corresponding to $R_{i\mathrm{top}}$;
$V_{i\mathrm{top}}$ — vehicle speed corresponding to $R_{i\mathrm{top}}$;
$\beta_{i\mathrm{top}}$ — trajectory angle corresponding to $R_{i\mathrm{top}}$;
$\Delta\theta_{i\mathrm{top}}$ — local pitch angle, for orbit transfer without inclination change, corresponding to $R_{i\mathrm{top}}$;
V_{sattop} — injection speed, for orbit transfer without inclination change, corresponding to $R_{i\mathrm{top}}$;
V_{cirtop} — speed in a circular orbit with ray equal to $R_{i\mathrm{top}}$;
$e_{\mathrm{orb\,max}}$ — maximum feasible eccentricity for a target orbit;
e_{orbIn} — target orbit eccentricity value, to be used in iterative procedures; and
$V_{\mathrm{sat\,min}}$ — minimum orbit injection speed for the target orbit, to be used in iterative procedures.

In the course of the suborbital trajectory, in normal conditions, there should be two points of same geocentric distance $R_{i\mathrm{bot}}$, one in the increasing altitude sector, the other in the decreasing altitude sector, where the impulsive transfer without inclination change (in relation to suborbital trajectory inclination) would lead to circular orbit with geocentric distance equal to $R_{i\mathrm{bot}}$. So, in points above those two of minimum ray $R_{i\mathrm{bot}}$ and up to the maximum impulse ray $R_{i\mathrm{top}}$ that in these normal conditions is the suborbital apogee ray R_{aposub} in Eq. (9), the transfer without inclination change would be by the perigee of the target orbit, in which the eccentricity would increase with the increasing of the impulse ray, to say, the target orbit perigee ray. And in points under those of minimum ray $R_{i\mathrm{bot}}$, the horizontal transfer would only be possible by the target orbit apogee, in which the eccentricity would increase with the decreasing of the impulse ray, to say, target orbit apogee ray.

Yet, in normal conditions, for each point above those of minimum ray $R_{i\mathrm{bot}}$, the introduction of orbit inclination change within the transfer would result in target orbit in which the eccentricity decreases with the increasing, in absolute value, of the orbit inclination change; up to attain null eccentricity, after what

the eccentricity would be increasing, but with transfer by apogee. If the inclination requirement is set preferential over the eccentricity requirement, the criterion here is to allow the quantification of inclination change up to the limit of circular resulting orbit. But, if the eccentricity requirement is set preferential over the inclination requirement, inclination change is quantified as to best fulfill the eccentricity requirement, with transfer by perigee. Note that the range of feasible solutions increases with the increasing of the altitude. Nevertheless, the solution that best fulfill the requirements, with priority, is associated to a unique feasible altitude. Moreover, if any of inclination value or eccentricity value results in its respective feasibility limit, the impulsive transfer is done at the highest possible altitude that, in the above normal conditions, is the suborbital apogee altitude h_{aposub}; and *vice versa*, if the impulsive transfer altitude results are the highest possible, at least one of the two requirements is quantified at its feasibility limit.

However, due to eventual severe dispersions, conditions might be diverse from the above. Examining Eq. (3), the minimum time interval from the initial time t_a to the impulse time t_i is $t_{\text{tip}} + t_{\text{cent}}$. If in this minimum time interval the vehicle is already above that minimum ray $R_{i\text{bot}}$, but not beyond the suborbital apogee ($Dt_a t_{\text{aposub}} \geq t_{\text{tip}} + t_{\text{cent}}$), then, if the impulse ray R_i is unfeasible in the increasing altitude sector, it is enough to make the transfer with R_i in the decreasing altitude sector.

Now, if in the minimum time interval the vehicle is already beyond suborbital apogee ($Dt_a t_{\text{aposub}} < t_{\text{tip}} + t_{\text{cent}}$), yet above the minimum ray $R_{i\text{bot}}$ in the decreasing altitude sector, the maximum impulse ray $R_{i\text{top}}$ becomes smaller than the suborbital apogee ray R_{aposub}. Hence, feasible solutions range becomes more constrained.

In the most adverse conditions, if the suborbital trajectory is such that it is not possible any transfer by the perigee of the target orbit, or if in the minimum time interval $t_{\text{tip}} + t_{\text{cent}}$ the vehicle is already under the minimum ray $R_{i\text{bot}}$ in the decreasing altitude sector, then the orbit transfer is accomplished at the greatest possible ray $R_{i\text{top}}$, without inclination change, with horizontal orbit injection, that in this case means by the apogee of the resulting orbit.

Using the results from Eqs. (1), (2), (6)–(11), (16), and (17), one has the following procedure.

1. If $E_a < \pi$ (vehicle in the increasing altitude sector) and $Dt_a t_{\text{aposub}} \geq t_{\text{tip}} + t_{\text{cent}}$:

$$E_{i\text{top}} = \pi\,; \tag{18}$$

$$R_{i\text{top}} = R_{\text{aposub}}\,; \tag{19}$$

$$Dt_a t_{i\text{top}} = Dt_a t_{\text{aposub}}\,; \tag{20}$$

$$f_{i\text{top}} = \pi\,; \quad \Delta\theta_{j\text{top}} = 0\,; \quad V_{\text{sattop}} = V_{\text{aposub}} + \Delta V_p\,.$$

2. Else, if $E_a \geq \pi$ or $Dt_a t_{\text{aposub}} < t_{\text{tip}} + t_{\text{cent}}$, the eccentric anomaly $E_{i\text{top}}$ is calculated first, using the time interval $\Delta t = t_{\text{tip}} + t_{\text{cent}}$, within the reference eccentric anomaly E_a; then, the remaining variables are calculated [2]:

$$E_{i\text{top}} = E_a + \frac{\Delta t \cdot n_{\text{sub}}}{1 - e_{\text{sub}} \cos(E_a)} ; \tag{21}$$

$$R_{i\text{top}} = a_{\text{sub}} \left(1 - e_{\text{sub}} \cos\left(E_{i\text{top}}\right)\right) ; \tag{22}$$

$$Dt_a t_{i\text{top}} = t_{\text{tip}} + t_{\text{cent}} ; \tag{23}$$

$$\cos\left(f_{i\text{top}}\right) = \frac{p_{\text{sub}} - R_{i\text{top}}}{e_{\text{sub}} R_{i\text{top}}} \rightarrow f_{i\text{top}} = 2\pi - \arccos\left(\cos\left(f_{i\text{top}}\right)\right) ;$$

$$V_{i\text{top}} = \left(\frac{2\mu}{R_{i\text{top}}} - \frac{\mu}{a_{\text{sub}}}\right)^{1/2} ; \quad \beta_{i\text{top}} = \arctan\left(\frac{e_{\text{sub}} \sin\left(f_{i\text{top}}\right)}{1 + e_{\text{sub}} \cos\left(f_{i\text{top}}\right)}\right) ;$$

$$\Delta\theta_{i\text{top}} = \arcsin\left(-\frac{V_{i\text{top}} \sin\left(\beta_{i\text{top}}\right)}{\Delta V_p}\right) ;$$

$$V_{\text{sattop}} = V_{i\text{top}} \cos\left(\beta_{i\text{top}}\right) + \Delta V_p \cos\left(\Delta\theta_{i\text{top}}\right) .$$

3. In a circular orbit of the ray $R_{i\text{top}}$, the speed is:

$$V_{\text{cirtop}} = \left(\frac{\mu}{R_{i\text{top}}}\right)^{1/2} .$$

Now, if one has $V_{\text{sattop}} \leq V_{\text{cirtop}}$, there are the most adverse conditions. Therefore, iterative procedures of subsections 2.5 and 2.6 are not applied and the time interval $Dt_a t_0$, true anomaly f_i, local pitch angle $\Delta\theta_i$, and local yaw angle ψ_V will be as follows:

$$Dt_a t_0 = Dt_a t_{i\text{top}} - t_{\text{cent}} ; \tag{24}$$

$$f_i = f_{i\text{top}} ; \tag{25}$$

$$\Delta\theta_i = \Delta\theta_{i\text{top}} ; \tag{26}$$

$$\psi_V = 0 . \tag{27}$$

If, instead, $V_{\text{sattop}} > V_{\text{cirtop}}$, there is a set of solutions, with transfer by the perigee of the target orbit. Aiming correct convergence, some feasibility bounds are set to be used within the iterations. The maximum feasible eccentricity corresponds to the transfer at the maximum ray, with no inclination change [2]:

$$e_{\text{orb max}} = \frac{V_{\text{sattop}}^2 R_{i\text{top}}}{\mu} - 1 .$$

Then, the target orbit eccentricity e_{orbIn}, to be used in iterations, may be smaller than the required e_{orb}. The minimum injection speed $V_{\mathrm{sat\,min}}$ relates to transfer at maximum ray [2], with inclination change set by the priority:

$$e_{\mathrm{orbIn}} = \begin{cases} e_{\mathrm{orb}} & \text{if } e_{\mathrm{orb}} \le e_{\mathrm{orb\,max}}\,; \\ e_{\mathrm{orb\,max}} & \text{if } e_{\mathrm{orb}} > e_{\mathrm{orb\,max}}\,; \end{cases} \tag{28}$$

$$V_{\mathrm{sat\,min}} = \begin{cases} \left(\dfrac{\mu}{R_{i\mathrm{top}}}\right)^{1/2} & \text{if the priority is inclination}\,; \\ \left(\dfrac{\mu(1+e_{\mathrm{orbIn}})}{R_{i\mathrm{top}}}\right)^{1/2} & \text{if the priority is eccentricity}\,. \end{cases} \tag{29}$$

The orbit requirements are on inclination and eccentricity. But the orbit injection speed corresponding to the required inclination depends upon the yet unknown declination at the point of impulsive transfer. Hence, it is not yet known if the limit $V_{\mathrm{sat\,min}}$ is going to impose inclination value different from the one required during iterations.

Furthermore, if inclination is the priority over eccentricity, the solution to be found for the inclination may cause to eccentricity greater constraint than that caused by $e_{\mathrm{orb\,max}}$.

The iterative procedures solve these issues.

2.5 Impulse Ray, Timing, and Local Pitch Angle

Figure 2 is a vector sketch of the impulsive transfer, with the following data referred to the impulse time t_i, vectors expressed in the frame **I**:

$\mathbf{R}_i$ — impulse ray ($R_i = \| \mathbf{R}_i \|$);

$\mathbf{V}_i$ — vehicle velocity in the suborbital trajectory ($V_i = \| \mathbf{V}_i \|$);

β_i — trajectory angle in the suborbital trajectory;

$\Delta\theta_i$ — local pitch angle, around vehicle's pitch axis, in plane **ZI**–**XI**, starting from **ZI**, negative if downward;

ψ_V — after angular displacement $\Delta\theta_i$, local yaw angle, around vehicle's yaw axis;

$\Delta\mathbf{V}_p$ — velocity increment, or characteristic velocity, due to propulsion ($\Delta V_p = \| \Delta\mathbf{V}_p \|$);

$\mathbf{V_{sat}} = \mathbf{V}_i + \Delta\mathbf{V}_p$ — target orbit injection velocity ($V_{\mathrm{sat}} = \| \mathbf{V}_{\mathrm{sat}} \|$); and

$\Delta\mathrm{Az}_i$ — azimuth change in the transfer.

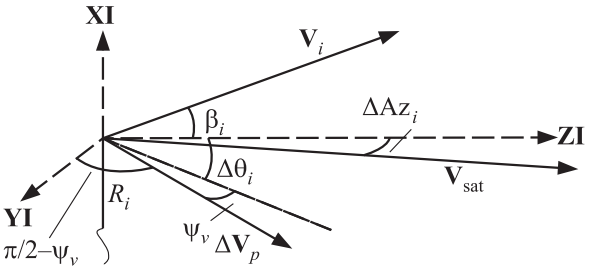

Figure 2 Vector diagram of the impulsive orbit transfer

2.5.1 Primary determination of the impulse ray

Still using the reference frame **I**, the following expressions hold for the velocities:

$$\mathbf{V}_i = V_i \left(\sin(\beta_i)\ 0\ \cos(\beta_i)\right)^{\mathrm{T}}\ ; \tag{30}$$

$$\Delta\mathbf{V}_p = \Delta V_p \left(\cos(\psi_V)\sin(\Delta\theta_i)\ \sin(\psi_V)\ \cos(\psi_V)\cos(\Delta\theta_i)\right)^{\mathrm{T}}\ ; \tag{31}$$

$$\mathbf{V}_{\mathrm{sat}} = \mathbf{V}_i + \Delta\mathbf{V}_p \rightarrow V_{\mathrm{sat}}^2 = V_i^2 + \Delta V_p^2 + 2\mathbf{V}_i\Delta\mathbf{V}_p\,. \tag{32}$$

The energy and angular momentum equations that hold for the suborbital trajectory are applied for the time t_i [3]:

$$V_i^2 - \frac{2\mu}{R_i} = -\frac{\mu}{a_{\mathrm{sub}}}\,; \tag{33}$$

$$V_i R_i \cos(\beta_i) = H_{\mathrm{sub}}\,. \tag{34}$$

If the orbit injection velocity $\mathbf{V}_{\mathrm{sat}}$ is to be in the local horizontal plane, then:

$$V_i \sin(\beta_i) + \Delta V_p \cos(\psi_V)\sin(\Delta\theta_i) = 0\,; \tag{35}$$

$$\left(V_i\cos(\beta_i) + \Delta V_p\cos(\psi_V)\cos(\Delta\theta_i)\right)^2 + \left(\Delta V_p \sin(\psi_V)\right)^2 = V_{\mathrm{sat}}^2\,. \tag{36}$$

If the target orbit eccentricity is e_{orbIn}, given by Eq. (28), with R_i becoming its perigee distance, then [2]:

$$V_{\mathrm{sat}}^2 = \frac{\mu(1+e_{\mathrm{orbIn}})}{R_i}\,. \tag{37}$$

The manipulation of Eqs. (30) to (37), aiming the determination of R_i, leads to the following 3rd-order equation [3]:

$$R_i^3 + A_1 R_i^2 + A_2 R_i + A_3 = 0\,. \tag{38}$$

Here,

$$A_1 = -\frac{2(3 + e_{\text{orbIn}})}{F};$$

$$A_2 = \frac{(3 + e_{\text{orbIn}})^2 + 4(\Delta V_p \sin(\psi_V) H_{\text{sub}}/\mu)^2}{F^2};$$

$$A_3 = -\frac{4H_{\text{sub}}^2(1 + e_{\text{orbIn}})}{\mu F^2}$$

where $F = 1/a_{\text{sub}} + \Delta V_p^2/\mu$; ΔV_p is the flight parameter predetermined as in Eq. (1); and a_{sub} and H_{sub} are given by Eqs. (7) and (5). The local yaw angle ψ_V is determined in the following subsection 2.6, but using the value of R_i now being determined. Hence, in the first iteration, a null value for ψ_V is used here. In successive iterations, ψ_V and R_i are alternately and iteratively calculated, the output of each iteration being the input to the next, till some condition is fulfilled; for instance, the differences between the outputs of consecutive iterations fall bellow certain negligible maxima. But, as the procedures are set here, a determination of R_i should be the first and the last one. Mathematically, Eq. (38) may have either one or three real roots, but only one should have feasible physical meaning. Let take the auxiliary variables $P = (A_1^2 - 3A_2)/9$; $Q = (9A_1A_2 - 2A_1^3 - 27A_3)/54$; and the three situations below [4]:

(1) $Q^2 - P^3 \cong 0$: All the three roots are real, the second one duplicate:

$$R_i = \begin{cases} 2Q^{1/3} - \dfrac{A_1}{3}; \\ -Q^{1/3} - \dfrac{A_1}{3}; \end{cases}$$

(2) first situation does not hold and $Q^2 - P^3 > 0$: one root is real:

$$R_i = \left(Q + \left(Q^2 - P^3\right)^{1/2}\right)^{1/3} + \left(Q - \left(Q^2 - P^3\right)^{1/2}\right)^{1/3} - \frac{A_1}{3};$$

(3) first situation does not hold and $Q^2 - P^3 < 0$: all three roots are real:

$$R_i = \begin{cases} 2P^{1/2}\cos\left(\dfrac{S}{3}\right) - \dfrac{A_1}{3}; \\ 2P^{1/2}\cos\left(\dfrac{S}{3} + \dfrac{2\pi}{3}\right) - \dfrac{A_1}{3}; \\ 2P^{1/2}\cos\left(\dfrac{S}{3} + \dfrac{4\pi}{3}\right) - \dfrac{A_1}{3} \end{cases} \tag{39}$$

where $S = \arccos(Q/P^{3/2})$.

In the above first and third situations, the solution should be selected by testing the physical meaning, for instance, which is the closest to a preestablished reasonable value. Nevertheless, in all cases simulated, the third situation holds and its last root listed in Eq. (39) is the solution.

2.5.2 Timing, fault conditions, and impulse ray adjustment

Using $E_{i\text{top}}$ (either Eq. (18) or Eq. (21)), $R_{i\text{top}}$ (either Eq. (19) or Eq. (22)), $Dt_at_{i\text{top}}$ (either Eq. (20) or Eq. (23)), E_a (Eq. (16)), a_{sub} (Eq. (7)), e_{sub} (Eq. (6)), n_{sub} (Eq. (11)), t_{cent} (Eq. (2)), and tipping time t_{tip}, one may set possible adjustment in the impulse ray R_i, eccentric anomaly E_i, and time interval Dt_at_i, from the initial time t_a to the impulse time t_i. There are two situations possible:

(1) $R_i \geq R_{i\text{top}}$ (fault: insufficient energy; this may occur even with the previous proceedings in subsection 2.4): Transfer at the maximum impulse ray: $E_i = E_{i\text{top}}$, $R_i = R_{i\text{top}}$, $Dt_at_i = Dt_at_{i\text{top}}$; and

(2) $R_i < R_{i\text{top}}$: E_i is calculated, at first, for increasing altitude [2]: $E_i = \arccos((a_{\text{sub}} - R_i)/(a_{\text{sub}}e_{\text{sub}}))$.

Then, Dt_at_i is calculated [2]:

$$Dt_at_i = \frac{1}{n_{\text{sub}}}\left\{E_i - E_a - e_{\text{sub}}\left[\sin(E_i) - \sin(E_a)\right]\right\} . \tag{40}$$

If results $Dt_at_i < t_{\text{tip}} + t_{\text{cent}}$ (fault: insufficient time in the increasing altitude sector), then E_i is recalculated for the decreasing altitude sector [3]: $E_i = 2\pi - E_i$. Then, Dt_at_i is recalculated as in Eq. (40). If yet results $Dt_at_i < t_{\text{tip}} + t_{\text{cent}}$ (fault: insufficient time in the decreasing altitude sector), then the transfer is at the maximum impulse ray: $E_i = E_{i\text{top}}$, $R_i = R_{i\text{top}}$, $Dt_at_i = Dt_at_{i\text{top}}$.

For both situations above, the time interval Dt_at_0, from initial time t_a to start-up time t_0, is finally calculated:

$$Dt_at_0 = Dt_at_i - t_{\text{cent}} . \tag{41}$$

2.5.3 Local pitch angle, orbit injection speed, and effective eccentricity

Using R_i, E_i, p_{sub} (Eq. (8)), e_{sub} (Eq. (6)), and a_{sub} (Eq. (7)), the true anomaly f_i, the vehicle speed V_i, and the trajectory angle β_i are determined at impulse time t_i [2]:

$$\cos(f_i) = \frac{p_{\text{sub}} - R_i}{e_{\text{sub}}R_i} ; \tag{42}$$

$$V_i = \left(\frac{2\mu}{R_i} - \frac{\mu}{a_{\text{sub}}}\right)^{1/2} ; \quad \beta_i = \arctan\left(\frac{e_{\text{sub}}\sin(f_i)}{1 + e_{\text{sub}}\cos(f_i)}\right)$$

where

$$\text{if } E_i < \pi, \text{ then } 0 \leq f_i < \pi; \text{ else } \pi \leq f_i < 2\pi\,.$$

If impulse ray R_i has been modified, then the target orbit eccentricity is different from that used for R_i primary determination. Anyway, orbit injection is to be horizontal; hence, respectively from Eqs. (35) and (36), one has the local pitch angle and the target orbit injection speed:

$$\Delta\theta_i = \arcsin\left(-\frac{V_i \sin(\beta_i)}{\Delta V_p \cos(\psi_V)}\right)\,; \tag{43}$$

$$V_{\text{sat}} = \left(\left(V_i \cos(\beta_i) + \Delta V_p \cos(\psi_V)\cos(\Delta\theta_i)\right)^2 + \left(\Delta V_p \sin(\psi_V)\right)^2\right)^{1/2}\,. \tag{44}$$

The resulting effective eccentricity that is not needed in the procedures can be obtained simply for information [2]:

$$e_{\text{orbEf}} = \frac{V_{\text{sat}}^2 R_i}{\mu} - 1\,.$$

2.6 Azimuth Change and Local Yaw Angle

In subsection 2.5, with a previous value of the local yaw angle ψ_V, there were calculated the impulse ray R_i, the vehicle speed V_i, the trajectory angle β_i, the true anomaly f_i, the orbit injection speed V_{sat}, and the local pitch angle $\Delta\theta_i$. In this subsection, other values for the orbit injection speed and the local pitch angle are calculated, named, respectively, V_{satI} and $\Delta\theta_{i\text{I}}$, using and keeping unchanged the remaining variables above; and a new value for ψ_V is generated.

In the orbit transfer, there should be an inclination change from the suborbital inclination I_{sub} to the target orbit required inclination I_{orb}. This inclination change corresponds to an azimuth change ΔAz_i, from the suborbital azimuth Az_{e_i} at impulse time t_i to the target orbit azimuth Az_{f_i} at the same time, or $\Delta\text{Az}_i = \text{Az}_{f_i} - \text{Az}_{e_i}$; this depends on the geographical location of the transfer. As Fig. 2 shows and regarding that here the orbit injection speed is named V_{satI} instead of V_{sat}, to achieve this azimuth change, the vehicle should be pointed with local yaw angle ψ_V so that:

$$V_{\text{satI}} \sin\left(\Delta\text{Az}_i\right) = \Delta V_p \sin(\psi_V)\,. \tag{45}$$

2.6.1 Primary determination of the azimuth change

Figure 3 illustrates, for the position of a vehicle in a Keplerian trajectory, the right spherical triangle delimited by the equatorial plane, the local meridian

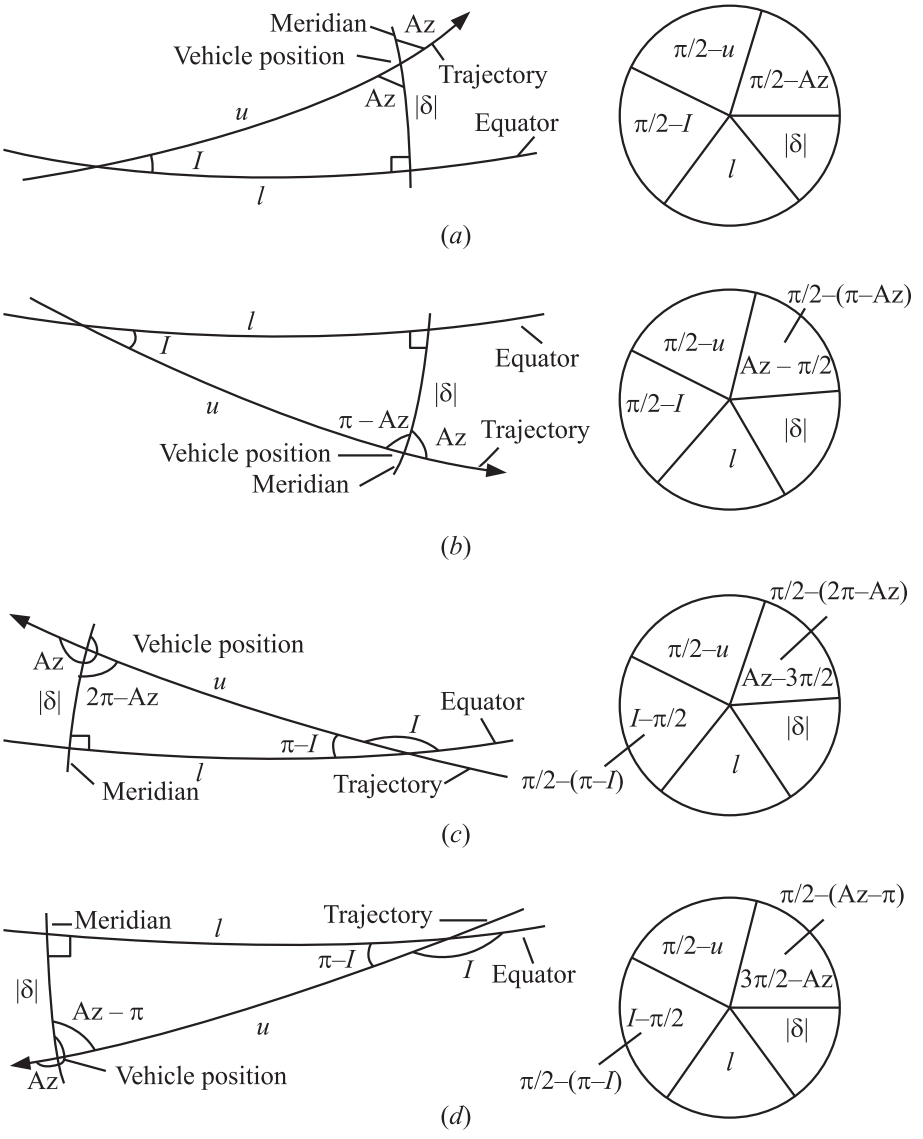

Figure 3 Trajectory spherical trigonometry: (*a*) $I < \pi/2$, vehicle at north hemisphere; (*b*) $I < \pi/2$, vehicle at south hemisphere; (*c*) $I > \pi/2$, vehicle at north hemisphere; and (*d*) $I > \pi/2$, vehicle at south hemisphere

plane, and the trajectory plane. Four situations are shown, varying the trajectory plane inclination that is in the range from 0 to π rad and the geographical position of the vehicle:

(a) inclination less than $\pi/2$ (progressive), and position at the north hemisphere;

(b) inclination less than $\pi/2$ (progressive), and position at the south hemisphere;

(c) inclination greater than $\pi/2$ (regressive), and position at the north hemisphere; and

(d) inclination greater than $\pi/2$ (regressive), and position at the south hemisphere.

In all the above situations, it should be noticed that the shown variables and expressions hold as well if the considered position is either in increasing latitude ($\pi/2 \leq u < \pi$, at the south hemisphere; $0 \leq u < \pi/2$, at the north hemisphere) or in decreasing latitude ($\pi/2 \leq u < \pi$, at the north hemisphere; $0 \leq u < \pi/2$, at the south hemisphere) sector of the trajectory. The concerning angular variables are:
$|\delta|$ (in the meridian plane) — absolute value of the declination at the current position;
l (in the equatorial plane) — equatorial angular displacement, from last equator crossing up to the current meridian;
I (between equatorial and trajectory planes) — trajectory plane inclination;
u (in the trajectory plane) — trajectory angular displacement, from last equator crossing up to the current position; and
Az (between meridian and trajectory planes) — trajectory current azimuth.

The circles for each situation in Fig. 3, suitably shared in the shown angles, are to guide the application of Napier rules [5] for right spherical triangles. So, there can be stated:

situation (a): $\sin(\pi/2 - I) = \cos(|\delta|)\cos(\pi/2 - \mathrm{Az})$;
situation (b): $\sin(\pi/2 - I) = \cos(|\delta|)\cos(\mathrm{Az} - \pi/2)$;
situation (c): $\sin(I - \pi/2) = \cos(|\delta|)\cos(\mathrm{Az} - 3\pi/2)$; and
situation (d): $\sin(I - \pi/2) = \cos(|\delta|)\cos(3\pi/2 - \mathrm{Az})$.

From any of these four statements results: $\sin(\mathrm{A}_z) = \cos(I)/\cos(|\delta|)$.

From the above value of its sine, the value of the azimuth is determined considering its corresponding quadrant that is determined by the inclination type (either $I < \pi/2$ or $I > \pi/2$), and by the trajectory sector of current position (either in increasing latitude sector or in decreasing latitude sector). Table 1 presents the azimuth determination in relation to the inclination type and the latitude variation related sector.

Table 1 Azimuth determination

Inclination type	Latitude variation	Azimuth quadrant	Azimuth Az
$I < \frac{\pi}{2}$	Increasing	1st	$\arcsin\left(\frac{\cos(I)}{\cos(\lvert\delta\rvert)}\right)$
	Decreasing	2nd	$\pi - \arcsin\left(\frac{\cos(I)}{\cos(\lvert\delta\rvert)}\right)$
$I > \frac{\pi}{2}$	Decreasing	3rd	$\pi - \arcsin\left(\frac{\cos(I)}{\cos(\lvert\delta\rvert)}\right)$
	Increasing	4th	$2\pi + \arcsin\left(\frac{\cos(I)}{\cos(\lvert\delta\rvert)}\right)$

It is assumed that the transfer occurs in such a manner that, at the impulsive transfer position, if the latitude is either increasing or decreasing in the origin trajectory, then it also will be, respectively, either increasing or decreasing in the target trajectory. In eventual cases where it would be possible to choose between two opposed maneuvers that would lead to trajectories with the same inclination, this corresponds to the option for the maneuver with less azimuth change.

However, there is a constraint for the target orbit inclination I_{orb}, which should be such that the trajectory can attain the impulsive transfer latitude δ_i, the constraint that may also be deduced from the azimuth column in Table 1:

$$|\cos(I_{\text{orb}})| \leq \cos(|\delta_i|) \rightarrow |\delta_i| \leq I_{\text{orb}} \leq \pi - |\delta_i| \,.$$

In each iteration, the value of I_{orbIn} for the target orbit inclination, to use in place of I_{orb}, is then set as follows:

$$I_{\text{orbIn}} = \begin{cases} |\delta_i| & \text{if } I_{\text{orb}} < |\delta_i| \,; \\ I_{\text{orb}} & \text{if } |\delta_i| \leq I_{\text{orb}} \leq \pi - |\delta_i| \,; \\ \pi - |\delta_i| & \text{if } I_{\text{orb}} > \pi - |\delta_i| \,. \end{cases} \tag{46}$$

After the above precaution, Table 2 presents the possible transfer cases with corresponding azimuth changes.

Examining Table 2, one concludes that the cosine and the sine of the azimuth change are, respectively:

$$\cos(\Delta \text{Az}_i) = \cos\left(\arcsin\left(\frac{\cos(I_{\text{orbIn}})}{\cos(|\delta_i|)}\right) - \arcsin\left(\frac{\cos(I_{\text{sub}})}{\cos(|\delta_i|)}\right)\right) ; \tag{47}$$

Table 2 Orbit transfer cases and azimuth changes

Latitude	Inclination		Azimuth change $\Delta \mathrm{A}_{z_i} = \mathrm{Az}_{f_i} - \mathrm{Az}_{e_i}$
	Origin	Target	
Increasing	$I_{\mathrm{sub}} < \frac{\pi}{2}$	$I_{\mathrm{orbIn}} < \frac{\pi}{2}$	$\arcsin\left(\frac{\cos(I_{\mathrm{orbIn}})}{\cos(\lvert\delta_i\rvert)}\right) - \arcsin\left(\frac{\cos(I_{\mathrm{sub}})}{\cos(\lvert\delta_i\rvert)}\right)$
	$I_{\mathrm{sub}} > \frac{\pi}{2}$	$I_{\mathrm{orbIn}} > \frac{\pi}{2}$	
	$I_{\mathrm{sub}} < \frac{\pi}{2}$	$I_{\mathrm{orbIn}} > \frac{\pi}{2}$	$2\pi + \arcsin\left(\frac{\cos(I_{\mathrm{orbIn}})}{\cos(\lvert\delta_i\rvert)}\right) - \arcsin\left(\frac{\cos(I_{\mathrm{sub}})}{\cos(\lvert\delta_i\rvert)}\right)$
	$I_{\mathrm{sub}} > \frac{\pi}{2}$	$I_{\mathrm{orbIn}} < \frac{\pi}{2}$	$\arcsin\left(\frac{\cos(I_{\mathrm{orbIn}})}{\cos(\lvert\delta_i\rvert)}\right) - 2\pi - \arcsin\left(\frac{\cos(I_{\mathrm{sub}})}{\cos(\lvert\delta_i\rvert)}\right)$
Decreasing	Any	Any	$-\arcsin\left(\frac{\cos(I_{\mathrm{orbIn}})}{\cos(\lvert\delta_i\rvert)}\right) + \arcsin\left(\frac{\cos(I_{\mathrm{sub}})}{\cos(\lvert\delta_i\rvert)}\right)$

$$\sin(\Delta \mathrm{Az}_i) = \pm \sin\left(\arcsin\left(\frac{\cos(I_{\mathrm{orbIn}})}{\cos(\lvert\delta_i\rvert)}\right) - \arcsin\left(\frac{\cos(I_{\mathrm{sub}})}{\cos(\lvert\delta_i\rvert)}\right)\right) \tag{48}$$

where the positive sign applies if the transfer is in increasing latitude and the negative sign applies if it is in decreasing latitude. To determine whether it is increasing or decreasing, let the variable U_i be the vehicle angular displacement from the last virtual transition by the least latitude position ($\pi/2$ rad before the ascending node) up to impulsive transfer position, in the suborbital trajectory; and check the value of U_i. This translates to:

$$U_i = \left(\frac{\pi}{2} + \omega_{\mathrm{sub}} + f_i\right) \text{modulo}\,(2\pi)\,;$$
$$\text{if } U_i \leq \pi \rightarrow \text{ transfer in increasing latitude}\,,$$
$$\text{else } \rightarrow \text{ transfer in decreasing latitude}\,. \tag{49}$$

However, the value of $|\delta_i|$ is yet unknown. Getting back to Fig. 3 and applying once more a Napier rule [5], one gets:

$$\sin(|\delta|) = \begin{cases} \cos\left(\frac{\pi}{2} - I\right)\cos\left(\frac{\pi}{2} - u\right) & \text{for } I < \frac{\pi}{2}\,; \\ \cos\left(I - \frac{\pi}{2}\right)\cos\left(\frac{\pi}{2} - u\right) & \text{for } I > \frac{\pi}{2}\,. \end{cases}$$

As $|\delta|$ can only be in the 1st quadrant, from any of both above expressions yields:

$$|\delta| = \arcsin(\sin(I)\sin(u))\,.$$

So, letting the variable u_i be the vehicle angular displacement from the last virtual cross by the equator plane up to impulsive transfer position, in the sub-orbital trajectory, one has:

$$u_i = (\omega_{\text{sub}} + f_i)\text{modulo}\,(\pi)\,; \quad |\delta_i| = \arcsin(\sin(I_{\text{sub}})\sin(u_i))\,. \tag{50}$$

Resuming, the azimuth change ΔAz_i is obtained by means of Eqs. (46) to (50), where I_{sub}, ω_{sub}, and f_i are given, respectively, by Eqs. (12), (13), and (42), and I_{orb} is a known parameter.

2.6.2 Orbit injection velocity and azimuth adjustment

With the orbit injection velocity now named $\mathbf{V}_{\text{satI}}$ instead of $\mathbf{V}_{\text{sat}}$, and the local pitch angle now named $\Delta\theta_{i\text{I}}$ instead of $\Delta\theta_i$, one obtains from Eqs. (30)–(32):

$$V_{\text{satI}}^2 = V_i^2 + \Delta V_p^2 + 2V_i\Delta V_p\,[\sin(\beta_i)\cos(\psi_V)\sin(\Delta\theta_{i\text{I}}) + \cos(\beta_i)\cos(\psi_V)\cos(\Delta\theta_{i\text{I}})]\,. \tag{51}$$

Expressing the null vertical component of $\mathbf{V}_{\text{satI}}$, as in Eq. (35), and its component in **ZI**, one gets, respectively:

$$V_i\sin(\beta_i) + \Delta V_p\cos(\psi_V)\sin(\Delta\theta_{i\text{I}}) = 0 \tag{52}$$

where

$$\cos(\psi_V)\sin(\Delta\theta_{i\text{I}}) = -\frac{V_i\sin(\beta_i)}{\Delta V_p}\,;$$

and

$$V_{\text{satI}}\cos(\Delta\text{Az}_i) = V_i\cos(\beta_i) + \Delta V_p\cos(\psi_V)\cos(\Delta\theta_{i\text{I}}) \tag{53}$$

where

$$\cos(\psi_V)\cos(\Delta\theta_{i\text{I}}) = \frac{V_{\text{satI}}\cos(\Delta\text{Az}_i) - V_i\cos(\beta_i)}{\Delta V_p}\,.$$

Substituting Eqs. (52) and (53) into Eq. (51) and developing it, one comes to the 2nd-order equation in V_{satI}:

$$V_{\text{satI}}^2 - 2V_i\cos(\Delta\text{Az}_i)\cos(\beta_i)V_{\text{satI}} + V_i^2 - \Delta V_p^2 = 0\,. \tag{54}$$

The solutions for Eq. (54) and the condition for real solution are, respectively:

$$V_{\text{satI}} = V_i\cos(\Delta\text{Az}_i)\cos(\beta_i) \pm \left[V_i^2(\cos(\Delta\text{Az}_i))^2(\cos(\beta_i))^2 - V_i^2 + \Delta V_p^2\right]^{1/2}\,; \tag{55}$$

$$(\cos(\Delta\text{Az}_i))^2 \geq \frac{V_i^2 - \Delta V_p^2}{(V_i\cos(\beta_i))^2}\,. \tag{56}$$

If the cosine of ΔA_{z_i} given by Eq. (47) does not fulfill Eq. (56) which also means that the 2nd side of Eq. (56) can only be positive and that $\cos \Delta Az_i$ can only be positive, the following adjustments are made in the values of the cosine and of the sine of ΔAz_i, where the previous sign of the sine is preserved:

$$\cos(\Delta Az_i) = \frac{(V_i^2 - \Delta V_p^2)^{1/2}}{V_i \cos(\beta_i)} ;$$

$$\sin(\Delta Az_i) = \begin{cases} \sin\left(\arccos\left(\cos\left(\Delta Az_i\right)\right)\right) & \text{if } \sin(\Delta Az_i) \geq 0 ; \\ \sin\left(-\arccos\left(\cos\left(\Delta Az_i\right)\right)\right) & \text{else.} \end{cases}$$

After the above eventual adjustments, if Eq. (55) gives two distinct positive solutions, the criterion here is to select the solution closest to the value of V_{sat} given by Eq. (44). Now, if the selected value of V_{satI} is less than $V_{\text{sat min}}$ given by Eq. (29), then V_{satI} is adjusted and, according and using Eq. (54), ΔAz_i is also adjusted, yet preserving the current sign of its sine:

$$V_{\text{satI}} = V_{\text{sat min}} ;$$

$$\cos(\Delta Az_i) = \frac{V_{\text{satI}}^2 + V_i^2 - \Delta V_p^2}{2 V_i \cos(\beta_i) V_{\text{satI}}} ;$$

$$\sin(\Delta A_{z_i}) = \begin{cases} \sin(\arccos(\cos(\Delta Az_i))) & \text{if } \sin(\Delta Az_i) \geq 0 ; \\ \sin(-\arccos(\cos(\Delta Az_i))) & \text{else.} \end{cases}$$

2.6.3 Local yaw angle and effective inclination

From Eqs. (52) and (53), one obtains:

$$\Delta\theta_{i\text{I}} = \arctan\left(-\frac{V_i \sin(\beta_i)}{V_{\text{satI}} \cos(\Delta Az_i) - V_i \cos(\beta_i)}\right) .$$

Then, replacing $\Delta\theta_i$ with $\Delta\theta_{i\text{I}}$ in Eqs. (45) and (52), the local yaw angle ψ_V is determined:

$$\sin(\psi_V) = \frac{V_{\text{satI}} \sin(\Delta Az_i)}{\Delta V_p} ; \tag{57}$$

$$\cos(\psi_V) = -\frac{V_i \sin(\beta_i)}{\Delta V_p \sin(\Delta\theta_{i\text{I}})} . \tag{58}$$

The resulting effective inclination I_{orbEf} that is not needed in the procedures can be obtained simply for information, replacing I_{orbIn} with I_{orbEf} in Eqs. (47)–(49) that, after manipulation, yields:

$$I_{\text{orbEf}} = \arccos\left(\sin\left(\arcsin\left(\frac{\cos(I_{\text{sub}})}{\cos(|\delta_i|)}\right) \pm \Delta Az_i\right) \cos(|\delta_i|)\right)$$

where the positive sign applies if $U_i \leq \pi$; and the negative sign applies if $U_i > \pi$.

2.7 Angular Attitude in Navigation Reference System

In the frame **I**, the attitude at the time of transfer is expressed by the angles $\Delta\theta_i$ (either Eq. (26) or Eq. (43)) and ψ_V (either Eq. (27) or Eqs. (57) and (58)). Using the true anomalies f_i (either Eq. (25) or Eq. (42)) and f_a (Eq. (15)), one has the attitude expressed in frame **V**, with pitch angle θ_V and yaw angle the same ψ_V. Because it is considered as null attitude when the vehicle body frame is coincident with the inertial reference frame but, by convenience, $\Delta\theta_i$ was measured starting from **ZI** instead of **XI**, now an offset of $-\pi/2$ is introduced in the rotation around **YI** or **YV**. Thus,

$$\theta_V = \Delta\theta_i - (f_i - f_a) - \frac{\pi}{2}\,.$$

The vehicle longitudinal orientation in the frame **V** is:

$$\mathbf{L_V} = (\cos(\psi_V)\cos(\theta_V)\sin(\psi_V) \quad -\cos(\psi_V)\sin(\theta_V))^{\mathrm{T}}\,.$$

Using matrix **TGV** of Eq. (4), the longitudinal orientation is transformed to the navigation frame **G**:

$$\begin{aligned}\mathbf{L_G} &= (L_{\mathbf{Gx}}\ L_{\mathbf{Gy}}\ L_{\mathbf{Gz}})^{\mathrm{T}} \\ &= (\cos(\psi_{\mathbf{G}})\cos(\theta_{\mathbf{G}}) \quad \sin(\psi_{\mathbf{G}}) \quad -\cos(\psi_{\mathbf{G}})\sin(\theta_{\mathbf{G}}))^{\mathrm{T}} = \mathbf{TGV}\cdot\mathbf{L_V}\end{aligned}$$

where $\theta_{\mathbf{G}}$ and ψ_G are, respectively, the pitch and yaw attitude angles, referred to the frame **G**, to be used at the transfer time. The determination of their values, from the $\mathbf{L_G}$ components, is mission dependent and should be performed carefully to identify their correct quadrants. The vehicle should be pointed and stabilized at this attitude within the time interval Dt_at_0, set forth by either Eqs. (24) or (41).

3 SIMULATIONS

For testing purposes, a software prototype was built based on the developed pointing method. This prototype runs within an already existing launcher flight simulator, providing fair assessment conditions. Several test cases have been performed, using two launch missions, one with suborbital trajectory in decreasing latitude, the other in increasing latitude. Table 3 lists some characteristics of the suborbital trajectory and the last stage for each mission.

In all cases shown, iterations have been set to stop when, within two consecutive iterations, the difference between the respective impulse rays R_i is less than 10^{-4} km, and that between the respective local yaw angles ψ_V is less than

Table 3 Suborbital trajectory and last stage characteristics

Characteristics		Mission	
		M1	M2
Suborbital trajectory	Time-varying latitude	Decreasing	Increasing
	Inclination I_{sub}	13.6556°	14.6205°
	Specific angular momentum H_{sub}, km^2/s	30104.16	28361.37
	Initial ray R_a, km	6620.254	6660.724
	Apogee ray R_{aposub}, km	7197.389	7065.621
	Apogee altitude h_{aposub}, km	819.250	687.482
	Apogee declination δ_{aposub}	−6.1942°	+1.4733°
	Time to apogee $Dt_a t_{\text{aposub}}$, s	463.430	373.896
	Tipping time t_{tip}, s	60	60
Last stage	Centroid time of thrust acceleration profile t_{cent}, s	42.468	42.687
	Characteristic speed ΔV_p, km/s	3.376259	3.613275

10^{-4} rad. In Tables 4–7, the values presented as accomplished inclination and accomplished eccentricity are determined by the launcher flight simulator, in procedures after completion of the pointing method actuation.

Tables 4 and 5 show the cases in which the inclination and eccentricity requirements could be fully performed for variations on M1 and M2, respectively. For both M1 and M2, the initial ascending phases are configured to attain suborbital trajectory with inclination close to the respective required target orbit inclination, and in such conditions that, with the last stage, a circular orbit at a preestablished altitude is achieved. Thus, Tables 4 and 5 have eccentricity values close to zero. Except for cases M1a and M2a, each eccentricity value is set near the feasibility limit for the corresponding inclination value. Besides, cases M1b, M1f, M2b, and M2f have inclination values set close to the corresponding feasibility limits for null eccentricity. Compliance between effective values, given by the pointing prototype, and corresponding accomplished values, given by the launcher flight simulator, can be verified.

Tables 6 and 7 show the cases in which the inclination and eccentricity requirements could not be fully performed for variations on M1 and M2, respectively. Therefore, for each pair of inclination/eccentricity requirements, two tests results are shown, with the priority set, respectively, to one and the other requirement. The effective values may differ from the corresponding required values according to the feasibility conditions and the chosen priority. In cases M1aI, M1aE, M2aI, and M2aE, the required inclination is unfeasible, regardless of the priority and the required eccentricity, whereas the required eccentricity may be feasible depending on the priority setting and the required inclination. In cases M1bI, M1bE, M2bI, and M2bE, the required inclination may be fea-

Table 4 Cases involving variations of M1, without constraints acting

Characteristics	Case					
	M1a	M1b	M1c	M1d	M1e	M1f
Required/effective inclination I_{orbEf}	14°	7°	10°	14°	18°	22°
Accomplished inclination	14.00°	7.00°	10.01°	14.01°	18.00°	22.00°
Required/effective eccentricity e_{orbEf}	0	0	0.02	0.03	0.02	0
Accomplished eccentricity	0.00053	0.00065	0.01993	0.02995	0.01996	0.00068
Impulsive transfer altitude h_i, km	743.104	808.673	807.530	815.235	811.564	816.788
Impulsive transfer declination δ_i	−4.9637°	−5.7441°	−5.7201°	−5.9179°	−5.8110°	−5.9781°
Azimuth change ΔAz_i	+0.3694°	−8.4022°	−4.2044°	+0.3817°	+4.6868°	+8.9111°
Iterations	3	13	6	3	6	9

Table 5 Cases involving variations of M2, without constraints acting

Characteristics	Case					
	M2a	M2b	M2c	M2d	M2e	M2f
Required/effective inclination I_{orbEf}	14°	6°	10°	14°	18°	24°
Accomplished inclination	14.00°	6.00°	10.00°	14.00°	18.00°	24.00°
Required/effective eccentricity e_{orbEf}	0	0	0.02	0.03	0.02	0
Accomplished eccentricity	0.00044	0.00055	0.01988	0.02987	0.01987	0.00061
Impulsive transfer altitude h_i, km	614.174	675.186	678.620	684.898	670.314	685.971
Impulsive transfer declination δ_i	+0.1511°	+0.9351°	+1.0166°	+1.2269°	+0.8370°	+1.2849°
Azimuth change ΔAz_i	+0.6205°	+8.6643°	+4.6372°	+0.6228°	−3.3842°	−9.4025°
Iterations	3	7	5	3	5	7

sible depending on the priority setting and the required eccentricity, whereas the required eccentricity is unfeasible, regardless of the priority setting and the required inclination. In cases M1cI, M1cE, M2cI, and M2cE, both requirements are unfeasible, regardless of the priority setting and the value of the other requirement. Examining the effective and accomplished values, one can verify that a requirement set with priority is fully performed if it is feasible, and that it is performed up to a feasibility limit if it is not feasible. The results also verify that a requirement not set with priority is at least partially performed provided the value of the other requirement does not achieve its feasibility limit. When

Table 6 Cases involving variations of M1, with constraints acting

Characteristics	Case					
	M1aI	M1aE	M1bI	M1bE	M1cI	M1cE
Required inclination I_{orb}	0°	0°	10°	10°	180°	180°
Required eccentricity e_{orb}	0.01	0.01	0.90	0.90	0.90	0.90
Priority (inclination/ eccentricity)	Inc	Ecc	Inc	Ecc	Inc	Ecc
Effective inclination I_{orbEf}	6.9390°	7.7741°	10°	I_{sub}	22.0980°	I_{sub}
Accomplished inclination	6.94°	7.78°	10.01°	13.66°	22.10°	13.66°
Effective eccentricity e_{orbEf}	0	0.01	0.02443	0.03171	0	0.03171
Accomplished eccentricity	0.00073	0.00995	0.02437	0.03166	0.00072	0.03166
Impulsive transfer altitude	h_{aposub}	h_{aposub}	h_{aposub}	h_{aposub}	h_{aposub}	h_{aposub}
Impulsive transfer declination	δ_{aposub}	δ_{aposub}	δ_{aposub}	δ_{aposub}	δ_{aposub}	δ_{aposub}
Azimuth change ΔAz_i	-9.0601°	-7.4869°	-4.32786°	0°	$+9.0601^\circ$	0°
Iterations	3	3	3	2	3	2

Table 7 Cases involving variations of M2, with constraints acting

Characteristics	Case					
	M2aI	M2aE	M2bI	M2bE	M2cI	M2cE
Required inclination I_{orb}	0°	0°	10°	10°	180°	180°
Required eccentricity e_{orb}	0.01	0.01	0.90	0.90	0.90	0.90
Priority (inclination/ eccentricity)	Inc	Ecc	Inc	Ecc	Inc	Ecc
Effective inclination I_{orbEf}	5.2563°	6.8845°	10°	I_{sub}	24.0916°	I_{sub}
Accomplished inclination	5.26°	6.89°	10.00°	14.62°	24.09°	14.62°
Effective eccentricity e_{orbEf}	0	0.01	0.02367	0.03122	0	0.03122
Accomplished eccentricity	0.00063	0.00989	0.02355	0.03109	0.00064	0.03109
Impulsive transfer altitude	h_{aposub}	h_{aposub}	h_{aposub}	h_{aposub}	h_{aposub}	h_{aposub}
Impulsive transfer declination	δ_{aposub}	δ_{aposub}	δ_{aposub}	δ_{aposub}	δ_{aposub}	δ_{aposub}
Azimuth change ΔAz_i	9.5015°	7.8219°	4.6557	0°	-9.5015°	0°
Iterations	3	3	3	2	3	2

this feasibility limit is achieved by the requirement set with priority, the value of the other requirement corresponds to either null eccentricity (cases M1aI, M1cI, M2aI, and M2cI) or null inclination change (cases M1bE, M1cE, M2bE, and M2cE), depending on which of these is the requirement. Tables 6 and 7 also verify the compliance between the effective and the accomplished values. As set in subsection 2.4, when any requirement achieves its feasibility limit, the orbit transfer is performed at the highest possible altitude; in the cases shown

here, this is the respective suborbital apogee altitude h_{aposub}, once the minimum time to impulsive transfer $t_{\text{tip}} + t_{\text{cent}}$ is less than the time to suborbital apogee $Dt_a t_{\text{aposub}}$ in all cases.

4 CONCLUDING REMARKS

The simulations show compliance with the specifications set forth in the development of the pointing method described in this paper. The results of all tests, some of which are depicted here, present suitable precision. Because the developed algorithm is a critical application to run in flight, the following characteristics of the algorithm are stated:

(1) treating for any conditions in flight, including adverse conditions resulting from severe dispersions, with generation of solutions that address the safety and the best possible fulfillment of the requirements;

(2) convergence in iterative procedures is assured, with little processing; and

(3) the algorithm is versatile in requirements values setting, priority setting, and precision to be achieved that may be refined with no practical impact on the response time.

Studies on the subject continue, on an orbit transfer not necessarily by orbit perigee, as well as on the controllable last stage.

REFERENCES

1. Robbins, H. M. 1966. An analytical study of the impulsive approximation. *AIAA J.* 4(8):1417–23.
2. Bate, R. R., D. D. Mueller, and J. E. White. 1971. *Fundamentals of astrodynamics.* Dover Publications.
3. Leite Filho, W. C., and P. S. Pinto. 1998. Guidance strategy for solid propelled launchers. *J. Guidance Control Dyn.* 21(6):1006–9.
4. Franklin, P. 1958. *Marks mechanical engineer's handbook.* Ch. 2: Mathematics. McGraw-Hill.
5. Wertz, J. R. 1978. *Spacecraft attitude determination and control.* Kluwer Academic Publs.